JOURNAL OF SOLID STATE CHEMISTRY 99, 336–342 (1992)

Electronic and Silver Ionic Conductions in Perovskite and Related Oxides

YASUMICHI MATSUMOTO, KENJI FUNAKI, JUKICHI HOMBO, AND YORIYUKI OGAWA

Department of Applied Chemistry, Faculty of Engineering, Kumamoto University, Kumamoto 860, Japan

Received November 19, 1991; in revised form February 11, 1992; accepted February 11, 1992

Electronic and silver ionic conductivities in some silver-containing oxides with perovskite and related structures, such as $AgNbO_3$ (perovskite), $AgSbO_3$ (pyrochlore-related structure), and Ag-doped Bi–(Pb)–Sr–Ca–Cu–O-system superconductor, were measured by four-probe techniques using Pt electrodes and Ag-β''-Al_2O_3 electrodes with silver ionic conduction, respectively. Both $AgNbO_3$ and $AgSbO_3$ were n-type semiconductors and their electronic conductivities increased with an increase in the silver content. The electronic conductivity of $AgSbO_3$ was higher than that of $AgNbO_3$, due to the presence of a large amount of oxygen vacancies. Sb^{4+} and/or Sb^{3+} in $AgSbO_3$, and Nb^{4+} in $AgNbO_3$ will act as a donor. Silver ionic conductivities were always lower than the electronic conductivities brought about by the above donors for both $AgNbO_3$ and $AgSbO_3$ ceramics. The activation energies of silver ionic conductivity were in the ranges of 1.01–1.58, 0.78–0.90, and 0.94–1.12 eV for $AgNbO_3$, $AgSbO_3$, and Ag-doped Bi-system superconductors, respectively. The silver ion was assumed to move via the Ag sites in the bulk for $AgNbO_3$, but to move in the grain boundaries for $AgSbO_3$ and the Bi-system superconductor. The mechanisms of the electronic and silver ionic conductions are discussed for the present oxide ceramics.

Introduction

Perovskite and related oxides have many useful applications such as superconductors, dielectrics, catalysts and electrocatalysts, etc. The electrical properties of these oxides if they contain transition metals are dominated by the interaction between transition-metal ions and oxygen ions in the lattice (*1*). On the other hand, ionic conduction, especially oxygen anion conduction, will be controlled by the amount of oxygen vacancies, because oxygen ions will move via oxygen vacancies existing in the oxygen ion sites in the lattice (*2*). However, cationic conduction has been scarcely measured for these type oxides.

Ag^+ ion is well known as a mobile cation in various halide compounds. It was found that Ag^+ ion can move easily even in the Y–Ba–Cu–O-system superconductor ceramics which has a perovskite-like structure, although its ionic conductivity was low because of the low concentration of Ag^+ ion in the lattice (*3*). In this oxide, Ag^+ ions were considered to move via Cu sites in the grain boundaries. However, Ag^+ ionic conductivity and its mechanism are unknown for the silver perovskite and related oxides. In the present paper, Ag^+ ionic conductivities in the perovskite and related oxides, such as $AgNbO_3$, $AgSbO_3$, and Ag-doped Bi–(Pb)–Sr–Ca–Cu–O-system superconductor ceramics, were measured

0022-4596/92 $5.00

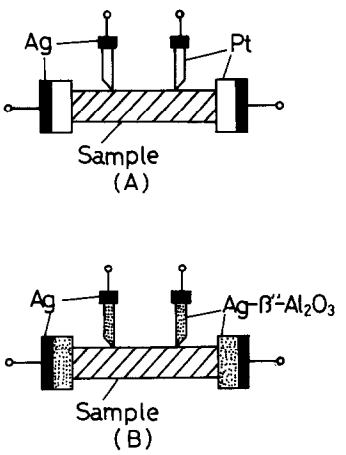

FIG. 1. Electrode setup for electronic (A) and Ag^+ ionic (B) conductivities.

by using a four-probe dc technique, and their mechanisms are discussed together with the electronic conduction mechanism.

Experimental

The Ag^+ ion conductivity and the electronic conductivities were measured by a four-probe dc technique with the experimental setup shown schematically in Fig. 1. Pt was used as the electrodes for the measurement of electronic conductivity (A), while Ag-β''-Al_2O_3 was used as the electrodes for the measurement of Ag^+ ion conductivity (B). The electrode of Ag-β''-Al_2O_3 was prepared by the same method as reported earlier (*4*, *5*). A constant current was applied between the current electrodes and the corresponding voltage drop was measured for both directions of the current flow.

Sb_2O_3, Nb_2O_5, and Ag_2O were used as the starting materials in the preparations of $AgNbO_3$ and $AgSbO_3$. The stoichiometrical mixtures were mixed and then calcined for 10 hr at 700°C. The powders were pressed into a tablet and then sintered at 700–1000°C for 24 hr. According to an X-ray diffraction analysis, small amounts of Ag metal were always present in both the $AgNbO_3$ perovskite (*6*) and the $AgSbO_3$ pyrochlore-related structure (*7*, *8*). PbO, Bi_2O_3, $CaCO_3$, $SrCO_3$, CuO, and Ag_2O were used as the starting materials in the preparation of the Ag-doped Bi–(Pb)–Sr–Ca–Cu–O-system superconductor. Four different mixtures with cationic compositions of $Bi_{1.4}Ag_{0.3}Pb_{0.3}Sr_2Ca_2Cu_3$, $Bi_{1.7}Pb_{0.3}Sr_{1.7}Ag_{0.3}Ca_2Cu_3$, $Bi_{1.7}Pb_{0.3}Sr_2Ca_{1.7}Ag_{0.3}Cu_3$, and $Bi_{1.7}Pb_{0.3}Sr_2Ca_2Cu_{2.7}Ag_{0.3}$ were heated at 800°C in air for 10 hr. The powders were then pressed into tablets, followed by sintering at 830°C for 10 hr in air. All the samples were mixtures consisted of 2212 and 2223 phases, except for the sample substituted nominally for Ca by Ag, which was a single phase of 2223. All the samples had a small amount of Ag metal.

Results and Discussion

Table I lists the particle size and the composition of bulk which was analyzed by electron probe microanalysis (EPMA), being compared with the nominal composition. The amount of Ag ion in the bulk (analytical composition) was always lower than that in the nominal composition for all the samples because of the production of free Ag metal, although analytical composition was close to the nominal composition for the samples heated at low temperatures (700°C for $AgSbO_3$ and 800°C for $AgNbO_3$). The values of x in $Ag_{n-x}SbO_3$ and $Ag_{n-x}NbO_3$ of the analytical compositions were about 0.03 except for the samples heated at low temperatures, if the nominal compositions are represented as Ag_nSbO_3 and Ag_nNbO_3. This indicates that the amounts of free Ag metal are always constant for all the samples heated at high temperatures. The amount of oxygen (y-value in Table I) was calculated from the weight loss during the productions of $AgNbO_3$ and $AgSbO_3$ from the starting materials in a thermal gravimetrical analysis (TG) and from the EPMA analysis. $AgSbO_3$

TABLE I

ANALYTICAL COMPOSITIONS AND PARTICLE SIZES OF $AgSbO_3$ AND $AgNbO_3$

Nominal composition	Heat-treatment temp. (°C)	Analytical composition	y-value	Particle size (μm)
$Ag_{0.95}SbO_3$	900	$Ag_{0.92}SbO_y$		0.9
$AgSbO_3$	700	$Ag_{1.00}SbO_y$		0.9
$AgSbO_3$	900	$Ag_{0.96}SbO_y$		1.3
			2.6 ± 0.3	
$Ag_{1.05}SbO_3$	900	$Ag_{1.04}SbO_y$		0.9
$Ag_{1.10}SbO_3$	900	$Ag_{1.07}SbO_y$		1.3
$Ag_{0.95}NbO_3$	1000	$Ag_{0.91}NbO_y$		6.8
$AgNbO_3$	800	$Ag_{0.99}NbO_y$		0.7
			2.95 ± 0.05	
$AgNbO_3$	1000	$Ag_{0.97}NbO_y$		6.7
$Ag_{1.05}NbO_3$	1000	$Ag_{1.02}NbO_y$		3.7
$Ag_{1.10}NbO_3$	1000	$Ag_{1.06}NbO_y$		3.9

had a much large amount of oxygen vacancies, compared with $AgNbO_3$, although the absolute values were not accurate for $AgSbO_3$. The oxygen release from the bulk was scarecely observed for the both samples in temperature region from 50 to 650°C, in the measurement of TG. In the case of $AgNbO_3$, the particle size increased by the heat-treatment at high temperature, as is shown in Table I.

Figures 2 and 3 show the electronic conductivities of $AgSbO_3$ and $AgNbO_3$ as a function of temperature; the measurements were performed by a four-probe technique using the apparatus (A) in Fig. 1. All the samples of $AgNbO_3$ and $AgSbO_3$ proved to be n-type semiconductors from the measurement of Seebeck coefficient. It was found that the electronic conductivities increased with an increase of the Ag content for both samples, as shown in these figures. Therefore, some cations with lower valence than Sb^{5+} or Nb^{5+} in the cases of stoichiometric compounds will exist in the bulk and will act as a donor.

There are two parts in the conductivity of $AgSbO_3$ as shown in Fig. 2. One is the intrinsic conduction at temperature range higher than about 450°C, and the other is the impurity conduction due to the donor at temperature range lower than 450°C. Both the conductions increase with an increase of the Ag content and saturate at $n = 1.0$ in

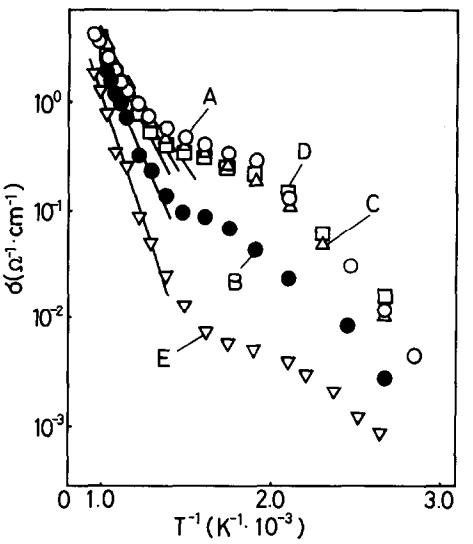

FIG. 2. Electronic conductivities of the $AgSbO_3$ system as a function of temperature (A) $AgSbO_3$ heated at 900°C; (B) $AgSbO_3$ heated at 700°C; (C) $Ag_{1.05}SbO_3$; (D) $Ag_{1.10}SbO_3$; and (E) $Ag_{0.95}SbO_3$.

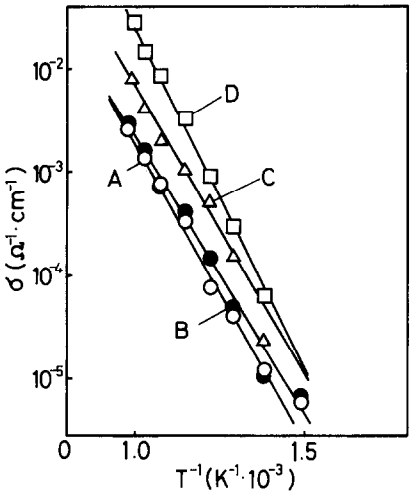

FIG. 3. Electronic conductivities of the $AgNbO_3$ system as a function of temperature: (A) $AgNbO_3$ heated at 1000°C; (B) $AgNbO_3$ heated at 800°C; (C) $Ag_{1.05}NbO_3$; and (D) $Ag_{1.10}NbO_3$.

Ag_nSbO_3. The bandgap which was calculated from the activation energy in the intrinsic conduction (Table II), decreased from 1.76 eV (n = 0.95) to 1.14 ± 0.02 eV (n = 1.0, 1.05, 1.10). The increase of the electronic impurity conduction with an increase of the Ag content will be based on the increase of Sb^{4+} and/or Sb^{3+} as a donor. The electron as a carrier will be produced by the following reactions:

$$Sb^{4+} \rightarrow Sb^{5+} + e^- \quad (1)$$

$$Sb^{3+} \rightarrow Sb^{5+} + 2e^-. \quad (2)$$

Therefore, the saturation of electronic impurity conductivity will be based on a saturation in the total concentration of above donors due to the increase in the oxygen vacancy as well as Ag^+ ion in the lattice, although the measurement of the accurate amount of oxygen was impossible with the present methods. Figure 4 shows the conductivities of $AgSbO_3$ and $AgNbO_3$ at 500°C as a function of the analytical Ag content ($n - x$).

The intrinsic electronic conductivity of $AgNbO_3$ also increased with an increase in the Ag content, but did not saturate as shown in Figs. 3 and 4. The conductivity of $Ag_{0.95}NbO_3$ was too low to be measured ($<10^{-5}\,\Omega^{-1}\,cm^{-1}$). Thus, the electronic conductivity of $AgNbO_3$ strongly depends on the Ag content. Their bandgaps calculated from the activation energy (Table II) were

TABLE II

ACTIVATION ENERGIES OF ELECTRONIC AND SILVER IONIC CONDUCTIVITIES

Nominal composition	Heat-treatment temp. (°C)	Activation energy of electrical conductivity (eV)	Activation energy of silver ionic conductivity (eV)
$Ag_{0.95}SbO_3$	900	0.88 (>450°C)	0.89
$AgSbO_3$	700	0.77 (>550°C)	0.88
$AgSbO_3$	900	0.58 (>550°C)	0.78
$Ag_{1.05}SbO_3$	900	0.56 (>500°C)	0.83
$Ag_{1.10}SbO_3$	900	0.57 (>500°C)	0.90
$AgNbO_3$	800	1.03	1.01
$AgNbO_3$	1000	1.10	1.15
$Ag_{1.05}NbO_3$	1000	1.11	1.35
$Ag_{1.10}NbO_3$	1000	1.34	1.58
$Bi_{1.4}Ag_{0.3}Pb_{0.3}Sr_2Ca_2Cu_3O_y$	830		0.94
$Bi_{1.7}Pb_{0.3}Sr_{1.7}Ag_{0.3}Ca_2Cu_3O_y$	830		1.12
$Bi_{1.7}Pb_{0.3}Sr_2Ca_{1.7}Ag_{0.3}Cu_3O_y$	830		1.07
$Bi_{1.7}Pb_{0.3}Sr_2Ca_2Cu_{2.7}Ag_{0.3}O_y$	830		1.04

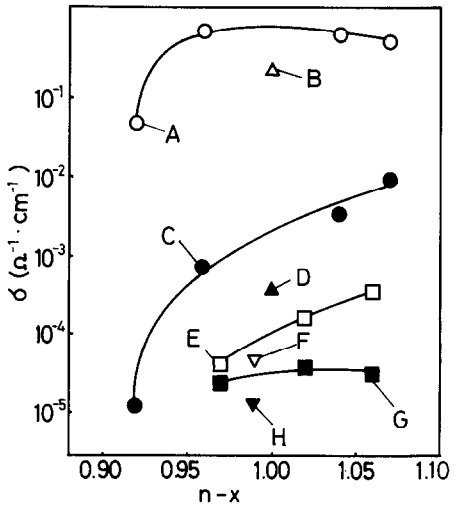

FIG. 4. Electronic (A, B, E, F) and Ag^+ ionic conductivities (C, D, G, H) at 500°C as a function of the analytical Ag content ($n - x$): (A, C) $AgSbO_3$ system heated at 900°C; (B, D) $AgSbO_3$ heated at 700°C; (E, G) $AgNbO_3$ system heated at 1000°C; and (F, H) $AgNbO_3$ heated at 800°C.

in the range from 2.06 to 2.68 eV. Probably, the amount of oxygen vacancy will be independent of the Ag content, and the concentration of Nb^{4+} as a donor will increase only with an increase in the Ag content. However, the concentration of the donor in Ag NbO_3 is very small compared with $AgSbO_3$, leading to low conductivity and no dominant impurity conduction, since the bandgap of $AgNbO_3$ is larger than that of $AgSbO_3$ and the amount of oxygen vacancy in $AgNbO_3$ is very small (about 0.05 as listed in Table I), compared with $AgSbO_3$ (about 0.4 as listed in Table I).

Figures 5 and 6 show the Ag^+ ionic conductivities in $AgSbO_3$ and $AgNbO_3$ as a function of temperature, respectively. The Ag^+ ionic conductivities are lower than their electronic conductivities for both samples, as shown in Fig. 4. The Ag^+ ionic conductivity of $Ag_{0.95}NbO_3$ was too low to be measured ($<10^{-5}\ \Omega^{-1}\ cm^{-1}$). The Ag^+ ionic conductivities of $AgSbO_3$ system were much higher than those of $AgNbO_3$, and increased with an increase in the Ag content. Thus, the amount of Ag^+ ion in the oxide strongly relates to the Ag^+ ionic conductivity. $AgSbO_3$ has a pyrochlore-related structure (7) which is a distorted perovskite structure and there is a large amount of oxygen vacancies in the samples we have used. It is now supposed that distortion in the structure in the cause that the Ag^+ ionic conductivity of $AgSbO_3$ is higher than that of $AgNbO_3$.

The Ag^+ ionic conductivity in Fig. 6 is not strongly dependent on the grain size for $AgNbO_3$ which follows from a comparison of the samples heated at 800°C (0.7 μm) and 1000°C (6.7 μm), as listed in Table I. This indicates that the Ag^+ ionic conduction in $AgNbO_3$ occurs in the bulk, and not in the grain boundaries, because the ionic conductivity depends on the particle size if the ionic conduction occurs in the grain boundaries (9). The activation energy of the Ag^+ ionic conductivity increases with an increase in

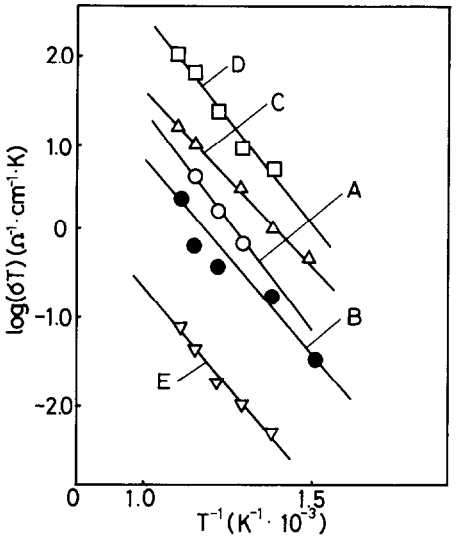

FIG. 5. Ag^+ ionic conductivities of the $AgSbO_3$ system as a function of temperature: (A) $AgSbO_3$ heated at 900°C; (B) $AgSbO_3$ heated at 700°C; (C) $Ag_{1.05}SbO_3$; (D) $Ag_{1.10}SbO_3$; and (E) $Ag_{0.95}SbO_3$.

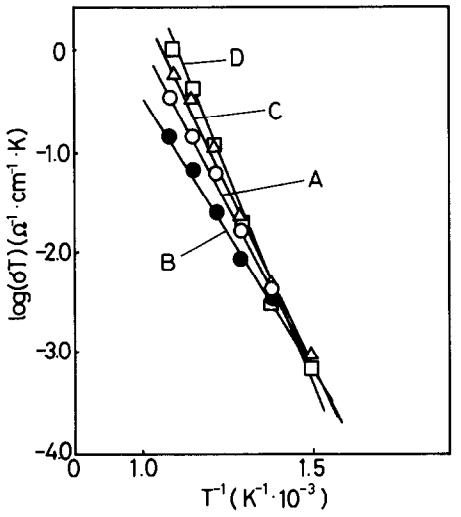

FIG. 6. Ag^+ ionic conductivities of the $AgNbO_3$ system as a function of temperature: (A) $AgNbO_3$ heated at 1000°C; (B) $AgNbO_3$ heated at 800°C; (C) $Ag_{1.05}NbO_3$; and (D) $Ag_{1.10}NbO_3$.

the Ag content, as shown in Fig. 6 and Table II. This suggests that for $AgNbO_3$, the Ag^+ ion will move easily via the Ag sites in the bulk containing some Ag vacancies.

On the other hand, it is not clear whether the Ag^+ ion moves in the bulk or grain boundaries for the $AgSbO_3$ sample, because the dependence of the conductivity on the particle size cannot be measured due to the independence of the particle size on the heat-treatment temperature (Table I). However, the independence of activation energy on the Ag content, as shown in Fig. 5 and Table II, may suggest that Ag^+ ions will move in the grain boundaries in the present $AgSbO_3$ samples. In this case, the Ag^+ ion will not move via regular crystallographic Ag sites, but via the disordered grain boundaries. The strong dependence of the Ag^+ ionic conductivity on the Ag content suggest that the amount of Ag^+ ions as carriers existing in the grain boundaries increases with an increase in the Ag content.

Figure 7 shows the Ag^+ ionic conductivity as a function of temperature in nominaly Ag-substituted Bi–(Pb)–Sr–Ca–Cu–O-system superconductors. According to an EPMA analysis, about 0.03 Ag ion (nominal content = 0.3 Ag) was doped in all the samples. Thus, the Ag^+ content was independent of the substituted elements. The activation energy was also independent of the substituted element and was always higher than those in $YBa_2Cu_3O_y$-system ceramics (*3*). The Ag^+ ionic conductivity was highest for the sample nominally substituted for Cu. Probably, the Ag^+ ion will also move via the Cu site in the grain boundaries in these Bi system ceramics similar to the case of the $YBa_2Cu_3O_y$ system. The higher activation energies of Ag^+ ionic conductivity for the Bi-system ceramics than for $YBa_2Cu_3O_y$-system ceramics indicates that the mobility of Ag^+ ion is lower for the Bi system than for $YBa_2Cu_3O_y$ system. Probably, this will be based on the shorter distance between the Cu–O planes for the Bi system than for $YBa_2Cu_3O_y$ system, which hampers the Ag-diffusion. The weak Ag-doped effect on the superconduction in the Bi-system supercon-

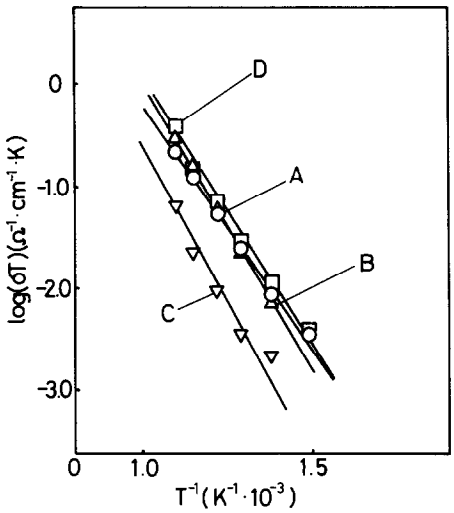

FIG. 7. Ag^+ ionic conductivities of Bi-system superconductors: (A) $Bi_{1.4}Ag_{0.3}Pb_{0.3}Sr_2Ca_2Cu_3O_y$; (B) $Bi_{1.7}Pb_{0.3}Sr_{1.7}Ag_{0.3}Ca_2Cu_3O_y$; (C) $Bi_{1.7}Pb_{0.3}Sr_2Ca_{1.7}Ag_{0.3}Cu_3O_y$; and (D) $Bi_{1.7}Pb_{0.3}Sr_2Ca_2Cu_{2.7}Ag_{0.3}O_y$.

ductor (*10*), compared with the case of $YBa_2Cu_3O_y$ system (*11*), will be based on the low mobility of the Ag^+ ion in its grain boundaries.

Summary

Electronic conductivities and silver ionic conductivities of $AgSbO_3$, $AgNbO_3$, and the Ag-doped Bi–(Pb)–Sr–Ca–Cu–O superconductor system were measured by a four-probe dc technique using Pt and Ag-β-Al_2O_3 electrodes, respectively. Both $AgSbO_3$ and $AgNbO_3$ were n-type semiconductors, and their electronic conductivities increased with an increase of the Ag content. Sb^{4+} and/or Sb^{3+} for $AgSbO_3$, and Nb^{4+} for Ag NbO_3 are supposed to act as a donor. The higher conductivity of $AgSbO_3$ than Ag NbO_3 is based on its smaller bandgap and the presence of large amount of oxygen vacancies which will produce high carrier density in $AgSbO_3$. Bandgaps were in the range from 1.76 to 1.14 eV for $AgSbO_3$, and from 2.68 to 2.08 eV for $AgNbO_3$. The silver ionic conductivity was also higher for $AgSbO_3$ than $AgNbO_3$, because of the distortion in structure for $AgSbO_3$. The silver ionic conduction is assumed to occur in the grains for $AgNbO_3$, and to occur in the grain boundaries for $AgSbO_3$ and the Bi superconductor system. The activation energies for the silver ionic conduction were 0.78–0.90 eV for $AgSbO_3$, 1.01–1.58 eV for $AgNbO_3$, and 0.94–1.12 eV for the Bi system. The higher activation energies for the Bi-system superconductor than for the $YBa_2Cu_3O_y$ superconductor indicates that the mobility of the silver ion is lower for the Bi system than for $YBa_2Cu_3O_y$.

References

1. J. B. Goodenough, *J. Appl. Phys.* **37,** 1415 (1966).
2. Y. Teraoka, H. M. Zhang, K. Okamoto, and N. Yamazoe, *Mater. Res. Bull.* **23,** 51 (1988).
3. Y. Matsumoto, Y. Yamaguchi, J. Hombo, T. Hauber and W. Göpel, submitted for publication.
4. M. S. Whittingham and R. A. Huggins, *J. Electrochem. Soc.* **116,** 1 (1971).
5. M. Breiter, M. Maly-Schreiber, and B. Dunn, *Solid State Ionics* **18–19,** 658 (1986).
6. M. Verwerft, D. Van Dyck, V. A. M. Brabers, J. Van Landuyt, and S. Amelinckx, *Phys. Status Solidi A* **112,** 451 (1989).
7. A. W. Sleight, *Mater. Res. Bull.* **4,** 377 (1969).
8. X. Turrillas, G. Delabouglise, and J. C. Joubert, *Solid State Ionics* **21,** 195 (1986).
9. S. Shirasaki, I. Shindo, and H. Haneda, *Chem. Phys. Lett.* **50,** 459 (1977).
10. Y. Matsumoto, J. Hombo, Y. Yamaguchi, and T. Mitsunaga, *Mater. Res. Bull.* **24,** 1469 (1989).
11. Y. Matsumoto, J. Hombo, and Y. Yamaguchi, *Mater. Res. Bull.* **24,** 1231 (1989).